Int. J. Heat Mass Transfer. Vol. 28, No. 9, pp. 1747–1755, 1985
Printed in Great Britain

0017-9310/85 $3.00 + 0.00
Pergamon Press Ltd.

On a model for frictioning stage in friction welding of thin tubes

A. FRANCIS
AWRE, Aldermaston, Reading, Berks RG7 4PR, U.K.

and

R. E. CRAINE
Faculty of Mathematical Studies, The University, Southampton SO9 5NH, U.K.

(*Received* 26 *July* 1984 *and in final form* 19 *March* 1985)

Abstract—The softened material that is present during the frictioning stage of the continuous drive friction welding process is modelled as a Newtonian fluid of large (but constant) viscosity. Axial shortening is included and approximate solutions, appropriate to thin tubes of mild steel, are found using the heat balance integral method.

1. INTRODUCTION

FRICTION welding is now used throughout the world as a reliable and automated welding process. Several variations of friction welding now exist [1] but in all cases the components to be joined are forced to rub against each other and the frictional heat generated at the rubbing interface softens the nearby material (the frictioning stage). After some time the rubbing is terminated and the weld is produced by solid-phase bonding in the hot material (the forging stage). We shall assume that the components to be joined are tubular and that the relative motion is a simple rotation (the continuous-drive welding process). The latter process has been considered in [2, 3], for example, and idealised traces are displayed in Fig. 1. In this paper we consider the evolution of the frictioning stage which is split into four phases.

Despite the importance of friction welding little progress has been made in constructing satisfactory theoretical models. Most authors have assumed in their models that heat is generated at the rubbing interface by sliding friction but, as the latter only occurs during Phase I (the conditioning phase) of the frictioning stage, the claims of these authors that their models hold throughout the welding cycle are clearly false. Moreover, none of the proposed forms for the frictional heating [4–9] seems consistent with the traces shown in

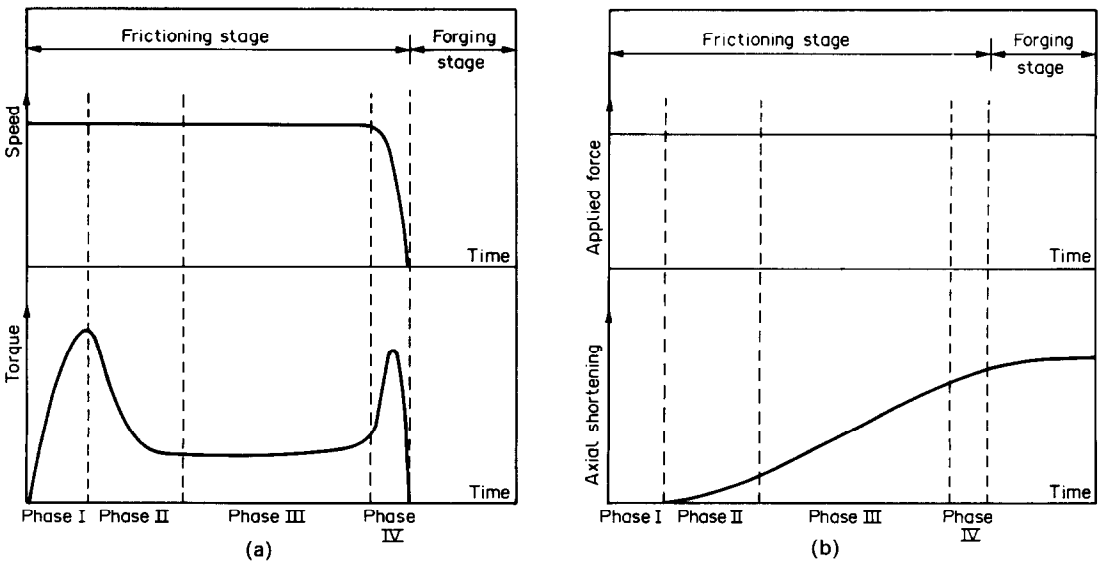

FIG. 1. Idealised traces for the continuous drive friction welding process. (a) Traces of speed and torque; (b) traces of applied force and axial shortening.

NOMENCLATURE

$a(t)$	coefficient in temperature profile (40)
Br	Brinkman number defined by (21a)
c_v	specific heat at constant volume
C_p	pressure coefficient defined by (18b)
$\mathbf{d}$	symmetric part of velocity gradient tensor, $\frac{1}{2}(\nabla\mathbf{v}+(\nabla\mathbf{v})^T)$
D/Dt	total time derivative
erfc(·)	complementary error function
$\mathbf{F}$	body force
F_o	Fourier number defined by (21c)
h	thickness of tube/plate
$\mathbf{I}$	unit tensor
k	thermal conductivity
p	pressure in plastic layer
Pe	Péclet number defined by (21b)
R	mean radius of tube
$R(\cdot)$	function defined by (48)
Re	Reynolds number defined by (18a)
$s(t)$	non-dimensional ratio, $\delta(t)/z_p(t)$
t	time
tr	trace
T	temperature
(u, v, w)	Cartesian components of velocity
$\mathbf{v}$	velocity
W_s	rate of axial shortening
(x, y, z)	Cartesian coordinates
$z_p(t)$	thickness of plastic layer.

Greek symbols

α	constant
β	non-dimensional ratio, h/z_{po}
γ	ratio defined by (18c)
$\delta(t)$	thickness of thermal layer in rigid region
η	independent variable, z/z_p
θ	non-dimensional temperature
μ	coefficient of viscosity
ρ	density
τ	shearing stress
ζ	independent variable, $z/z_{p\infty}$
ω	relative angular speed of rotation of tubes
∇	Nabla operator.

Subscripts

am	ambient
c	conditioning
o	reference value
s	value in rigid region
∞	equilibrium value.

Superscripts

$\bar{}$	superposed bar denotes dimensional quantity.

Fig. 1. The value of the theoretical work in [6] and [10] is also questionable since the authors assume that the rubbing interface reaches, and then remains at, the melting temperature even though experimental investigations [2, 11, 12] strongly suggest that melting never occurs.

Phase I ends (and Phase II begins) when the applied torque reaches its initial maximum value and the material near the rubbing interface is about to flow. In Phase II the material close to this interface gradually softens and heat is generated not through sliding friction at the interface but by mechanical dissipation throughout the softened (or plasticised) material. The applied axial load causes the softened material to flow radially outwards forming an upset collar with a consequential axial shortening of the components being joined. After a short time Phase III is reached; this is the equilibrium phase during which the torque, temperature distribution and rate of axial shortening all remain effectively constant. The rotating component is gradually brought to rest during Phase IV (or deceleration phase) by the application of a hydraulic brake and the frictioning stage is concluded when the rotation actually stops.

The central problem in modelling Phases II–IV concerns the choice of constitutive equation to describe the softened material. Healy *et al.* [13] have represented the material as a Bingham solid and obtained some results for Phase III (valid only for small Péclet numbers). The softened layer has also been modelled as a viscous fluid of large viscosity by Atthey [14], who found a similarity solution applicable to Phase II but with axial shortening completely omitted. Both models have been investigated further by Francis [15] who concludes, on the basis of his work, that the viscous fluid model is simpler to use and gives results which are in closer agreement with the traces in Fig. 1. In this paper, therefore, we adopt the viscous fluid model for the plasticised material and investigate in some detail Phases II and III of the frictioning stage for the friction welding of two thin tubes of steel. The results obtained are encouraging and we believe that our model increases our understanding of the underlying physical mechanisms and provides a sound basis for further work.

It is well known that the quality of a weld is significantly influenced by the thermal processing of the materials being joined. The temperature profiles calculated from a satisfactory theoretical model of the frictioning stage, for different input parameters,

therefore provide useful information to the experimentalist on assessing the strength of the welds that would be formed under those input conditions.

2. GOVERNING EQUATIONS FOR PHASES II AND III

The continuous-drive friction welding of two identical coaxial thin walled tubes of circular cross-section is considered. Both tubes have wall thickness $\bar{h}$ and mean radius $\bar{R}$ ($\bar{h} \ll \bar{R}$). In a real process one tube is stationary whilst the other rotates with constant angular speed ω. To simplify the analysis, however, we assume without loss of generality that the tubes rotate about their common axis, in opposite senses, with the same constant angular speed $\frac{1}{2}\omega$. As is customary in many similar situations we model each thin-walled tube as a semi-infinite plate of thickness $\bar{h}$. Cartesian axes $0\bar{x}\bar{y}\bar{z}$ are introduced as shown in Fig. 2 and the plates are assumed to move in the $\bar{y}$-direction with speeds $\pm\frac{1}{2}\omega\bar{R}$ respectively. Since our problem is axisymmetric we have $\partial/\partial\bar{y} \equiv 0$.

In this paper we concentrate on Phases II and III of the frictioning stage, modelling the softened material as an incompressible Newtonian fluid of large viscosity. The remaining part of each plate is represented as a rigid continuum. Under our assumptions the equations governing the motion of either plate can be written:

plastic layer

$$\operatorname{div} \bar{\mathbf{v}} = 0, \tag{1}$$

$$\frac{\mathrm{D}\bar{\mathbf{v}}}{\mathrm{D}\bar{t}} + \bar{\mathbf{F}} = \frac{1}{\bar{\rho}} \operatorname{div}(-\bar{p}\mathbf{I} + 2\bar{\mu}\mathbf{d}), \tag{2}$$

$$\bar{\rho}\bar{c}_{\mathrm{v}} \frac{\mathrm{D}\bar{T}}{\mathrm{D}\bar{t}} = 2\bar{\mu} tr(\mathbf{d})^2 + \operatorname{div}(\bar{k} \operatorname{grad} \bar{T}), \tag{3}$$

rigid region

$$\bar{\rho}_{\mathrm{s}}\bar{c}_{\mathrm{vs}} \frac{\mathrm{D}\bar{T}_{\mathrm{s}}}{\mathrm{D}\bar{t}} = \operatorname{div}(\bar{k}_{\mathrm{s}} \operatorname{grad} \bar{T}_{\mathrm{s}}). \tag{4}$$

(For a fuller discussion of this section the reader should consult [15].)

Suppose the Cartesian components of $\bar{\mathbf{v}}$ are $(\bar{u}, \bar{v}, \bar{w})$. Non-dimensional quantities are then introduced through the definitions

$$x = \bar{x}/\bar{h}, \quad z = \bar{z}/z_{\mathrm{po}}, \quad v = \bar{v}/(\tfrac{1}{2}\omega\bar{R}),$$
$$w = \bar{w}/w_{\mathrm{o}}, \quad t = \bar{t}/t_{\mathrm{o}}, \tag{5}$$

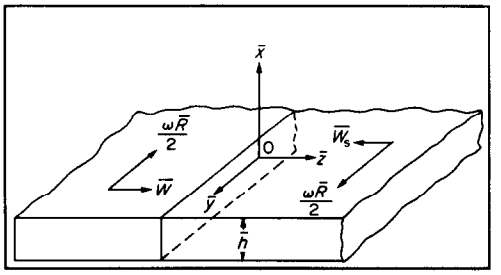

FIG. 2. Two-dimensional model of thin plates.

and recalling equation (1) we put

$$u = \bar{u}/(\beta w_{\mathrm{o}}), \quad \text{where } \beta = \bar{h}/z_{\mathrm{po}}. \tag{6}$$

Further, we define non-dimensional temperatures in the plastic and rigid regions by

$$\theta = (\bar{T} - \bar{T}_{\mathrm{am}})/(\bar{T}_{\mathrm{c}} - \bar{T}_{\mathrm{am}}), \quad \theta_{\mathrm{s}} = (\bar{T}_{\mathrm{s}} - \bar{T}_{\mathrm{am}})/(\bar{T}_{\mathrm{c}} - \bar{T}_{\mathrm{am}}). \tag{7}$$

Next we formulate in non-dimensional form some boundary conditions on the velocity and temperature. Symmetry implies

$$\frac{\partial u}{\partial z} = v = w = 0 \quad \text{on} \quad z = 0, \quad -\tfrac{1}{2} \leqslant x \leqslant \tfrac{1}{2}, \tag{8a, b, c}$$

whilst continuity of velocity at the plastic/rigid interface $z = z_{\mathrm{p}}$ leads to

$$u = 0, \quad v = 1, \quad w = -W_{\mathrm{s}}(t) \quad \text{on} \quad z = z_{\mathrm{p}}, \quad -\tfrac{1}{2} \leqslant x \leqslant \tfrac{1}{2}, \tag{9a, b, c}$$

where the rate of axial shortening of the rigid region, $\bar{W}_{\mathrm{s}}$, has been non-dimensionalised through

$$W_{\mathrm{s}} = \bar{W}_{\mathrm{s}}/w_{\mathrm{o}}. \tag{10}$$

Assuming that the position of the plastic/rigid interface is determined from the requirement that its temperature is always equal to the conditioning temperature $\bar{T}_{\mathrm{c}}$, we impose the condition

$$\theta = \theta_{\mathrm{s}} = 1 \quad \text{on} \quad z = z_{\mathrm{p}}, \quad -\tfrac{1}{2} \leqslant x \leqslant \tfrac{1}{2}. \tag{11}$$

For thin-walled tubes v varies only slightly with radius at the plastic/rigid interface. Moreover, a metallurgical examination of diametric cross-sections of welded tubes reveals that the temperature is virtually constant across such surfaces. It seems reasonable, therefore, to assume that v, θ and θ_{s} are all independent of x. Consistency with (11) then requires a similar assumption for z_{p} and, recalling (8c) and (9c), it follows that w is independent of x on both $z = 0$ and $z = z_{\mathrm{p}}$. As a result we postulate that w is independent of x everywhere, and hence throughout this work on thin-walled tubes assume

$$z_{\mathrm{p}} = z_{\mathrm{p}}(t), \quad v = v(z, t), \quad w = w(z, t),$$
$$\theta = \theta(z, t), \quad \theta_{\mathrm{s}} = \theta_{\mathrm{s}}(z, t). \tag{12}$$

With the further definitions

$$\mu = \bar{\mu}/\bar{\mu}_{\mathrm{o}}, \quad p = \bar{p}/p_{\mathrm{o}} \tag{13}$$

and the use of (5), (6) and (12), equations (1) and (2) can be written

$$\frac{\partial u}{\partial x} + \frac{\partial w}{\partial z} = 0 \tag{14}$$

$$\gamma\frac{\partial u}{\partial t} + u\frac{\partial u}{\partial x} + w\frac{\partial u}{\partial z} = -\frac{C_{\mathrm{p}}}{2\beta^2}\frac{\partial p}{\partial x} + \frac{1}{Re}\left[\frac{2}{\beta^2}\frac{\partial}{\partial x}\left(\mu\frac{\partial u}{\partial x}\right) + \frac{\partial}{\partial z}\left(\mu\frac{\partial u}{\partial z}\right)\right] \tag{15}$$

$$\gamma\frac{\partial v}{\partial t}+w\frac{\partial v}{\partial z}=\frac{1}{Re}\frac{\partial}{\partial z}\left(\mu\frac{\partial v}{\partial z}\right) \tag{16}$$

$$\gamma\frac{\partial w}{\partial t}+w\frac{\partial w}{\partial z}=-\frac{1}{2}C_p\frac{\partial p}{\partial z}+\frac{1}{Re}\left[\frac{\partial}{\partial x}\left(\mu\frac{\partial u}{\partial z}\right)+2\frac{\partial}{\partial z}\left(\mu\frac{\partial w}{\partial z}\right)\right] \tag{17}$$

where

$$Re=\frac{\bar{\rho}w_o z_{po}}{\mu_o},\quad C_p=\frac{p_o}{\frac{1}{2}\bar{\rho}w_o^2},\quad \gamma=\frac{z_{po}}{w_o t_o} \tag{18a,b,c}$$

and the small body force has been omitted.

Values for the parameters pertinent to thin tubes of mild steel are now introduced. Typically we have $\bar{R}=O(10^{-2})$ m, $\bar{h}=O(10^{-3})$ m, $\omega=O(10^2)$ rad s^{-1} and impose an applied axial force and applied torque per unit area of O(5) kN and O(10^2) kN m^{-1} respectively. Moreover, from real welds we observe that $w_o=O(10^{-3})$ m s^{-1}, $t_o=O(1)$ s and $z_{po}=O(10^{-3})$ m. It then follows that $\beta=O(1)$ and from considering the forces and torques acting on both ends of the rigid parts of the thin tubes we deduce that $p_o=O(10^8)$ N m^{-2} and $\mu_o=O(10^4)$ kg m^{-1} s^{-1}. Taking $\bar{\rho}=7800$ kg m^{-3} the appropriate values for the non-dimensional parameters (18) are $Re=O(10^{-6})$, $C_p=O(10^{10})$ and $\gamma=O(1)$ so the LHSs of equations (15)–(17) can all be neglected for our problem.

Turning to the energy equations (3) and (4) we assume, for simplicity, that $\bar{\rho}=\bar{\rho}_s$, $\bar{c}_v=\bar{c}_{vs}$, $\bar{k}=\bar{k}_s$ and that all these material coefficients are constant. Then, with the aid of (5)–(7), (12) and (13), equations (3) and (4) become:

plastic layer

$$\frac{\partial^2\theta}{\partial z^2}+Br\,\mu\left(\frac{\partial v}{\partial z}\right)^2=Pe\,w\frac{\partial\theta}{\partial z}+\frac{1}{F_o}\frac{\partial\theta}{\partial t} \tag{19}$$

rigid region

$$\frac{\partial^2\theta_s}{\partial z^2}=-Pe\,W_s\frac{\partial\theta_s}{\partial z}+\frac{1}{F_o}\frac{\partial\theta_s}{\partial t} \tag{20}$$

where

$$Br=\frac{\mu_o\omega^2\bar{R}^2}{4\bar{k}(\bar{T}_c-\bar{T}_{am})}, \tag{21a}$$

$$Pe=\frac{w_o\bar{z}_{po}}{(\bar{k}/\bar{\rho}\bar{c}_v)}, \tag{21b}$$

$$F_o=\frac{(\bar{k}/\bar{\rho}\bar{c}_v)}{(\bar{z}_{po}^2/t_o)}. \tag{21c}$$

Note that the term involving Br in equation (19) arises from the dominant term in the viscous dissipation. Typical values for $\bar{k}$ and $\bar{c}_v$ for mild steel are O(20) kg ms^{-3} K^{-1} and O(420) m^2 s^{-2} K^{-1} respectively and taking $\bar{T}_{am}=15$°C, $\bar{T}_c=700$°C and recalling the other numerical values introduced earlier, we deduce that in our situation $Br=O(1)$, $Pe=O(1)$ and $F_o=O(1)$. No further simplifications to equations (19) and (20) are therefore possible at this stage.

Let us now complete the set of boundary and initial conditions involving the velocity and temperature. For thin tubes approximately the same amounts of material are extruded from the inner and outer surfaces. Consequently, in our two-dimensional plate analogue we assume that $x=0$ is a plane of symmetry and require that

$$u(0,z,t)=0,\quad 0\leqslant z\leqslant z_p. \tag{22}$$

Symmetry of the temperature about $z=0$ and continuity of the heat flux at the plastic/rigid interface imply respectively that

$$\frac{\partial\theta}{\partial z}=0\quad\text{on}\quad z=0,\qquad \frac{\partial\theta}{\partial z}=\frac{\partial\theta_s}{\partial z}\quad\text{on}\quad z=z_p. \tag{23}$$

Over the time scales considered here heat transfer is only significant in the solid close to the plastic/rigid interface so it is reasonable to assume that

$$\theta_s(z,t)\to 0\quad\text{as}\quad z\to\infty. \tag{24}$$

Clearly heat is lost from the surfaces $x=\pm\frac{1}{2}$ by forced convection and radiation. However, these losses can be shown to be small compared with the heat conducted along the plates and are neglected in this paper.

Assuming that the applied axial force is constant throughout the frictioning stage (experimental observations suggest that this is a reasonable postulate), we deduce from a consideration of the forces acting on both ends of the rigid regions that the pressure in the plastic layer must satisfy the relation

$$\int_{-1/2}^{+1/2}\left(C_p\,Re\,p-4\mu\frac{\partial w}{\partial z}\right)dx=C_p\,Re\quad\text{on}\quad z=z_p. \tag{25}$$

At the end of Phase I no plasticised material has been formed and, recalling (12), we postulate that the initial conditions for Phase II are

$$z_p(0)=0,\quad \theta_s(z,0)=0, \tag{26a,b}$$

where time is measured from the beginning of Phase II. It should be emphasised that in a real weld the value of θ_s at the end of Phase I is non-zero. Nevertheless, assumption (26b) is adopted here since it simplifies the analysis and only affects the results for Phase II at small times (see [15]).

Solutions to equations (14), (15)–(17) (with the LHSs zero), (19) and (20) subject to the boundary conditions (8), (9), (11) and (22)–(25) and the initial conditions (26) are sought in the following sections.

3. PHASE II—SOLUTIONS AND RESULTS

In order to obtain an exact solution to the initial-boundary-value problem formulated in Section 2, Atthey [14] introduced the two further assumptions that no axial shortening takes place ($w=0$) and that the viscosity of the Newtonian fluid is constant ($\mu=1$). The solution of the simplified problem is then:

$$u=0,\quad v=\eta,\quad p=1 \tag{27}$$

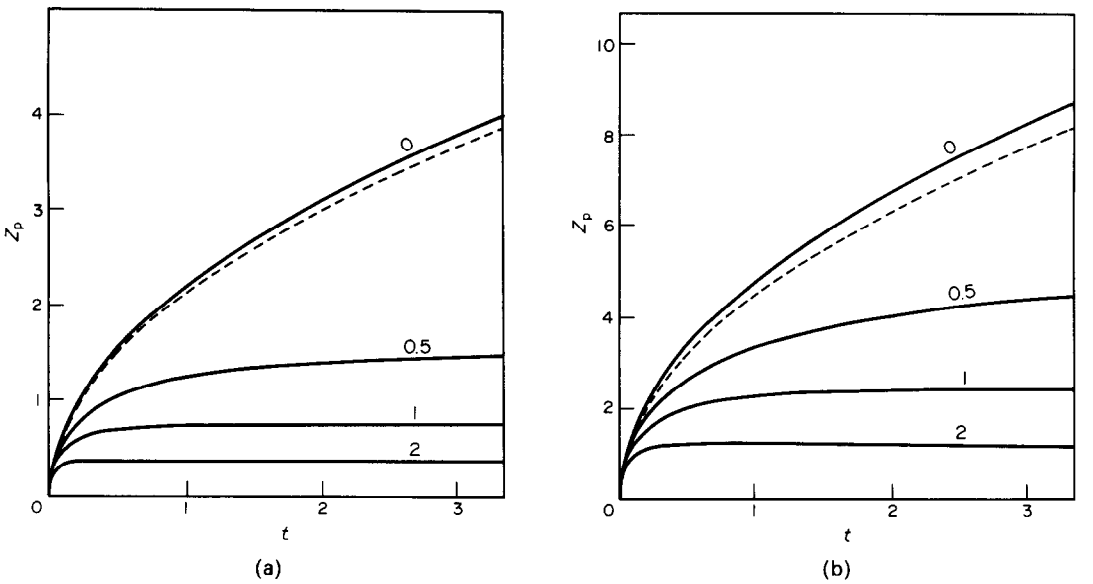

FIG. 3. Variation of thickness of plastic layer with time: ----- exact solution for $Pe = 0$ derived in Section 3; —— approximate solution obtained in Section 3 using heat balance integral method at stated values of Pe. (a) Plots for $Br = 1$; (b) plots for $Br = 5$.

$$\theta(\eta) = 1 + \frac{Br}{\alpha^2}\int_{\alpha\eta}^{\alpha} e^{-u^2}\left(\int_0^u e^{v^2}\,dv\right)du, \quad 0 \leqslant \eta \leqslant 1 \tag{28}$$

$$\theta_s(\eta) = \operatorname{erfc}(\alpha\eta)/\operatorname{erfc}(\alpha), \quad \eta \geqslant 1 \tag{29}$$

where

$$\eta = z/z_p, \quad z_p = 2\alpha(F_o t)^{1/2} \tag{30a, b}$$

and the constant α satisfies

$$2\alpha^2 = Br\,\pi^{1/2}\operatorname{erfc}(\alpha)\int_0^{\alpha} e^{v^2}\,dv. \tag{31}$$

(Note that equation (28) corrects an error of sign in equation (22) in [14].) Numerical solution of equation (31) for α allows us to calculate θ, θ_s and z_p from equations (28), (29) and (30b) and to determine the shearing stress τ from

$$\tau = \frac{\partial v}{\partial z} = z_p^{-1}. \tag{32}$$

Note that the stress is initially infinite with this model since $z_p(0) = 0$. Results for z_p, τ and the temperature (θ and θ_s) when $Br = 1$ and $Br = 5$ are shown by the dashed lines in Figs. 3–5.

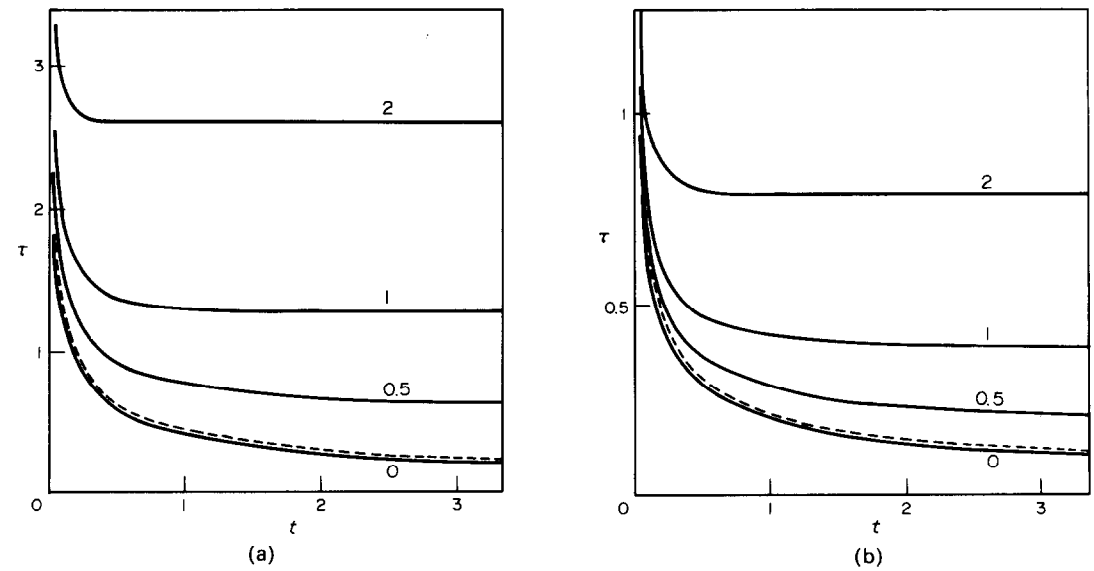

FIG. 4. Variation of shear stress with time: ----- exact solution for $Pe = 0$ derived in Section 3; —— approximate solution obtained in Section 3 using heat balance integral method at stated values of Pe. (a) Plots for $Br = 1$; (b) plots for $Br = 5$.

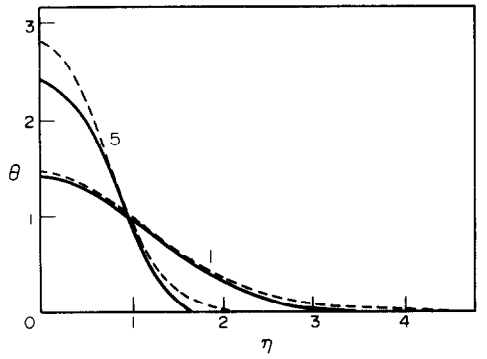

FIG. 5. Variation of temperature with non-dimensional distance at stated values of Br when $t = 1$: ----- exact solution for $Pe = 0$ derived in Section 3; —— approximate solution obtained in Section 3 using heat balance integral method.

Although the similarity solution stated above is fairly simple it is clear from (30b) (or Fig. 4) that the thickness of the plastic region increases indefinitely with time and from (28) and (29) that the temperature distribution throughout the plates, as a function of η, is independent of time. None of these results is observed in a real friction weld.

To remove the unrealistic features in the above solution we therefore include axial shortening (i.e. take $w \neq 0$), but retain all the other assumptions. We also observe from experiment that the rate of axial shortening, $\bar{W}_s$, is essentially constant throughout Phases II and III, provided that the applied force is kept constant. Hence, recalling the definition (10), we assume without loss of generality that $W_s = 1$. It is then straightforward to show that the solution of the reduced forms of equations (14)–(17) which satisfies conditions (8), (9) and (25) is

$$\left.\begin{aligned}(u, v, w) &= \left[\frac{3x}{2z_p}(1-\eta^2), \eta, \tfrac{1}{2}\eta(\eta^2-3)\right] \\ p &= 1 + 3(C_p Re)^{-1} \\ &\quad \times \left[\left(\frac{\beta}{z_p}\right)^2\left(\frac{1}{12}-x^2\right)+\eta^2-1\right]\end{aligned}\right\} \quad 0 \leqslant \eta \leqslant 1. \tag{33, 34}$$

As discussed in Section 2 the product $C_p\, Re$ is typically $O(10^4)$. With the aid of (33) the energy equations (19) and (20), for $\theta(\eta, t)$ and $\theta_s(\eta, t)$, can be written

$$\frac{\partial^2\theta}{\partial\eta^2} + Br = \frac{Pe}{2} z_p \eta(\eta^2-3)\frac{\partial\theta}{\partial\eta} + \frac{z_p^2}{F_o}\frac{\partial\theta}{\partial t} - \frac{z_p}{F_o}\frac{dz_p}{dt}\eta\frac{\partial\theta}{\partial\eta}, \quad 0 < \eta < 1 \tag{35}$$

$$\frac{\partial^2\theta_s}{\partial\eta^2} = -Pe\, z_p\frac{\partial\theta_s}{\partial\eta} + \frac{z_p^2}{F_o}\frac{\partial\theta_s}{\partial t} - \frac{z_p}{F_o}\frac{dz_p}{dt}\eta\frac{\partial\theta_s}{\partial\eta}, \quad \eta > 1 \tag{36}$$

and the boundary conditions (11), (23) and (24) become

$$\frac{\partial\theta}{\partial\eta}(0, t) = 0, \quad \theta(1, t) = \theta_s(1, t) = 1, \tag{37a, b, c}$$

$$\frac{\partial\theta}{\partial\eta}(1, t) = \frac{\partial\theta_s}{\partial\eta}(1, t), \quad \theta_s \to 0 \quad \text{as} \quad \eta \to \infty. \tag{38a, b}$$

It is clear from (26a) and (30a) that the initial condition (26b) also leads to (38b).

No analytical solution to equations (35) and (36) subject to (37) and (38) seems possible so we seek an approximate solution using the heat balance integral method (first proposed by Goodman [16]). To this end we first integrate equation (35) with respect to η from 0 to 1 and obtain, on using (37a),

$$\frac{\partial\theta}{\partial\eta}(1, t) + Br = \frac{Pez_p}{2}\int_0^1 \eta(\eta^2-3)\frac{\partial\theta}{\partial\eta}\,d\eta + \frac{z_p^2}{F_o}\frac{d}{dt}\int_0^1 \theta\,d\eta - \frac{z_p}{F_o}\frac{dz_p}{dt}\int_0^1 \eta\frac{\partial\theta}{\partial\eta}\,d\eta. \tag{39}$$

Next we postulate that θ can be approximated by a simple quadratic profile. The appropriate form which satisfies conditions (37a, b) is

$$\theta(\eta, t) = 1 - a(t)(1-\eta^2), \quad 0 \leqslant \eta \leqslant 1, \tag{40}$$

and substituting this expression into (39) and performing the necessary integrations we derive, after some algebra, the ordinary differential equation

$$2a + Br = -\frac{2z_p^2}{3F_o}\frac{da}{dt} - \frac{2z_p a}{3F_o}\frac{dz_p}{dt} - \frac{4Pez_p a}{5}. \tag{41}$$

In the rigid region we postulate (as in [16]) the existence of a thermal layer $z = \delta(t)$, where $\delta > z_p$, such that $\theta_s = 0$ when $z \geqslant \delta$. The latter implies that the heat flux across $z = \delta$ is also zero, therefore we can write

$$\theta_s(s, t) = \frac{\partial\theta_s}{\partial\eta}(s, t) = 0, \quad \text{where} \quad s(t) = \delta(t)/z_p(t). \tag{42}$$

On integrating equation (36) with respect to η from 1 to s and making use of conditions (37c) and (42) we derive the heat balance integral equation

$$-\frac{\partial\theta_s}{\partial\eta}(1, t) = Pez_p + \frac{z_p^2}{F_o}\frac{d}{dt}\int_1^s \theta_s\,d\eta - \frac{z_p}{F_o}\frac{dz_p}{dt}\int_1^s \eta\frac{\partial\theta_s}{\partial\eta}\,d\eta. \tag{43}$$

Assuming a quadratic profile for θ_s in $1 \leqslant \eta \leqslant s$ it is easily deduced that the form that satisfies our postulates and conditions (37c), (38a) and (42) is

$$\left.\begin{aligned}\theta_s &= a^2(s-\eta)^2, \quad s = 1 - a^{-1}, \quad 1 \leqslant \eta \leqslant s \\ \theta_s &= 0, \quad \eta \geqslant s.\end{aligned}\right\} \tag{44}$$

Substitution of the results (44) into equation (43), with the subsequent calculation of the integrals, then leads to

$$-2a = \frac{z_p^2}{3F_o a^2}\frac{da}{dt} + \frac{z_p}{F_o}\left(1 - \frac{1}{3}a^{-1}\right)\frac{dz_p}{dt} + Pe\, z_p. \quad (45)$$

The pair of ordinary differential equations (41) and (45) forms a coupled system for the two unknown functions $z_p(t)$ and $a(t)$.

No analytical solution to (41) and (45) is possible, but a numerical solution can be found using the Runge–Kutta forward step method (see [17], for instance). The numerical procedure is started by using the leading terms in the small time series solutions of (41) and (45). The values obtained by the Runge–Kutta process for z_p are used with equation (32) to give τ and both z_p and τ are plotted in Figs. 3 and 4 respectively for $Br = 1$ and $Br = 5$ at various values of the Péclet number. Knowledge of $a(t)$ enables the corresponding temperature profiles to be calculated from (40) and (44) and these calculations have been performed at times $t = 0.1$ and 1.0 for various values of the Péclet number in the range $0 \leqslant Pe \leqslant 2$. Since all these temperature profiles are closely similar only the profile for $Pe = 0$ is shown in Fig. 5.

The accuracy of the approximate solutions obtained with the heat balance integral method can be assessed in two ways. Firstly, when $Pe = 0$ Figs. 3–5 reveal fairly close agreement (especially at the lower value of Br) between the displayed approximate solutions and the corresponding exact ones derived from the formulae stated at the beginning of this section. Results at other values of Br confirm the closeness of the two sets of solutions particularly at small values of Br. Secondly, Francis [15] has developed series solutions valid for small times to the two pairs of equations (35), (36) and (41), (45). A detailed comparison of results derived from the first two terms in his series solutions indicates slight differences at very small times but the discrepancies decrease as t increases (although one recalls that t must remain 'small'). The above comments encourage us to believe that our solutions obtained for $Pe \neq 0$ by the heat balance integral method *are* reasonably accurate, except at very small times and when $Br \gg 1$.

It is clear from Figs. 3(a) and (b) that when axial shortening is included in our model the thickness of the plastic layer z_p always reaches some equilibrium value. Moreover, for given Br, this equilibrium thickness increases and is approached more rapidly as Pe increases. These trends are expected since as Pe increases more heat is lost by forced convection in the plastic layer and consequently less heat is available to increase the region's width. Figures 3(a) and (b) also reveal that for a given value of Pe an increase in Br leads both to a thicker plastic layer and a delay in the time needed to reach equilibrium.

The curves in Figs. 4(a) and (b) indicate the decay of τ with time and again equilibrium is obtained whenever $Pe \neq 0$. It should be remembered, however, that in our model τ is infinite when $t = 0$.

From the temperature profiles displayed in Fig. 5 we observe that an increase in the value of Br increases θ but decreases θ_s. A careful inspection of all the numerical results obtained with the heat balance integral method also reveals that the inclusion of axial shortening leads to a reduction in θ (a cooling due to forced convection) and that as t increases at a fixed value of Pe the temperature θ decreases (slightly) to its equilibrium value. The latter observation is unrealistic since in a real friction weld the temperature θ *rises* during Phase II to its equilibrium value.

It is important to note that apart from the small-time behaviour of τ and θ the results obtained with the heat balance integral method for $Pe \neq 0$ are qualitatively consistent with the idealised traces for Phase II shown in Fig. 1. Moreover, all additional results calculated using different values for the parameters confirm the general features of the solutions which have been stated above.

4. SOLUTION FOR PHASE III

In this section we determine the equilibrium solutions $z_{p\infty}$, θ_∞ and $\theta_{s\infty}$ to equations (35) and (36), the governing equations for our model. In equilibrium no explicit dependence on time occurs, so all time derivatives in (35) and (36) are zero and all partial derivatives with respect to η in (35) to (38) become ordinary derivatives. The solution to the simplified form of (36) which satisfies the conditions (37c) and (38b) is easily found to be

$$\theta_{s\infty} = \exp\left[-Pe\, z_{p\infty}(\zeta - 1)\right], \quad \text{where} \quad \zeta = z/z_{p\infty}. \quad (46)$$

Then obtaining the integrating factor for the reduced form of (35) and integrating twice with respect to ζ gives

$$\theta_\infty = 1 - Br\int_1^\zeta \exp\left[R(u)\right]\left(\int_0^u \exp\left[-R(v)\right]dv\right)du, \quad (47)$$

where the constants have been chosen to satisfy (37a, b) and we have introduced $R(\zeta)$ through

$$R(\zeta) = \frac{Pe\, z_{p\infty}}{8}\zeta^2(\zeta^2 - 6). \quad (48)$$

Substituting the solutions (46) and (47) into the remaining condition (38a) leads to

$$Br\exp\left[R(1)\right]\int_0^1 \exp\left[-R(\zeta)\right]d\zeta = Pe\, z_{p\infty}. \quad (49)$$

A numerical solution for $z_{p\infty}$ to the integral equation (49) is found using the Newton–Raphson iterative method and the computer results are plotted against Br in Fig. 6 for $Pe = 0.1, 0.5, 1$ and 5. Also displayed in this figure are the corresponding (equilibrium) values for $z_{p\infty}$ arising from the heat balance integral method discussed in Section 3. The two sets of solutions are in close agreement, especially when the values of Pe and Br are both less than 1.

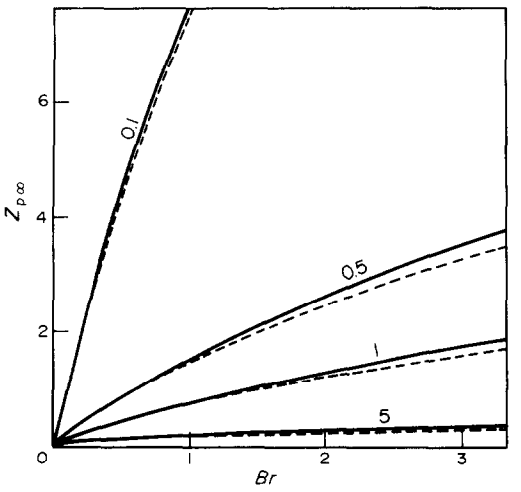

FIG. 6. Variation of thickness of plastic layer during Phase III with Br at stated values of Pe: ----- exact solution derived in Section 4; —— equilibrium solution arising from heat balance integral method obtained in Section 3.

5. CONCLUSION

In this paper we have considered the frictioning stage of the continuous-drive friction welding process, modelling the softened material in Phases II and III as a Newtonian fluid of large, but constant, viscosity. Attention has been confined to the welding of thin tubes and to simplify the analysis we have investigated the associated Cartesian problem involving two semi-infinite thin plates. Axial shortening has been included, enabling an equilibrium phase to be reached, and we have found a number of solutions for Phase II using the heat balance integral method, assuming Phase I to be absent. These approximate solutions have been shown to be reasonably accurate when comparison with exact ones is possible, and they possess many of the qualitative features of real welds. Moreover, the solutions have been found without the associated algebraic details becoming too complex. To complete the paper we have derived a number of equilibrium solutions appropriate to Phase III of the frictioning stage.

In a real friction weld the coefficient of viscosity varies with temperature and strain-rate and in order to reproduce experimental results it is necessary to include these effects into our model. Some simple models illustrating such variations have been investigated [15]. A proper consideration of the conditioning phase (Phase I) has also been given in [15], where it is shown that the inclusion of Phase I into the theoretical model ensures a more realistic small-time behaviour in the distribution of the temperature during Phase II. The heat balance integral method has proved sufficiently robust to include these additional complexities and a summary of these, and further, extensions will appear separately.

Representing the plastic layer as a Newtonian fluid has therefore enabled us to derive a number of solutions pertinent to the frictioning stage of the friction welding of thin tubes. Moreover, extensions currently in progress are producing encouraging results. A final assessment of the model's usefulness, however, must await a quantitative comparison with experimental traces and this cannot be achieved until we have a more detailed knowledge of the dependence of the material parameters (such as coefficient of viscosity) on temperature and strain rate.

Acknowledgements—The authors are indebted to Dr A. P. Bennett for helpful comments at various stages of this project. A.F. is also grateful to the Science Research Council and Marchwood Engineering Laboratories, CEGB for the award of a CASE studentship at Southampton University where this work was completed.

REFERENCES

1. Friction welding of butt joints in metals for high duty applications, British Standard 6223. British Standards Institution, London (1982).
2. F. D. Duffin and A. S. Bahrani, The mechanics of friction welding mild steel, *Metal Construct.* **8**, 267–271 (1976).
3. F. D. Duffin and A. S. Bahrani, Frictional behaviour of mild steel in friction welding, *Wear* **26**, 53–74 (1973).
4. V. I. Vill, *Friction Welding of Metals*. Reinhold, New York (1962).
5. V. I. Vill, Energy distribution in the friction welding of steel bars, *Weld. Prod.* **6**, 31–41 (1959).
6. T. Rich and R. Roberts, Thermal analysis for basic friction welding, *Metal Construct. Br. Weld. J.* **3**, 93–98 (1971).
7. N. N. Rykalin, A. J. Pugin and V. A. Vassiljeva, The heating and cooling of rods butt-welded by the friction process, *Weld. Prod.* **6**, 42–52 (1959).
8. A. S. Gel'dman and M. P. Sander, Power and heating in the friction welding of thick-walled steel pipes, *Weld. Prod.* **6**, 53–61 (1959).
9. V. D. Voznesenskii, Power and heat parameters of friction welding, *Weld. Prod.* **6**, 62–70 (1959).
10. C. J. Cheng, Transient temperature distribution during friction welding of two similar materials in tubular form, *Weld. J.* **41**, 542s–549s (1962).
11. I. F. Squires, Thermal and mechanical characteristics of friction welding mild steel, *Br. Weld. J.* **13**, 652–657 (1966).
12. L. G. Petrucci, Temperature distribution in friction welding, *Gen. Engr* **89**, 179–185 (1978).
13. J. J. Healy, D. J. McMullan and A. S. Bahrani, Analysis of frictional phenomena in friction welding of mild steel, *Wear* **37**, 265–278 (1976).
14. D. R. Atthey, A simple thermal analysis for friction welding, CEGB Electrical Research Memo. 549, Job. No. TB294, pp. 1–7 (1976).
15. A. Francis, Mathematical models for friction welding. Ph.D. thesis, University of Southampton (1983).
16. T. R. Goodman, The heat balance integral and its applications to problems involving a change of phase, *Trans. Am. Soc. mech. Engrs* **80**, 335–342 (1958).
17. R. J. Gould, R. F. Hoskins, J. A. Milner and M. J. Pratt, *Applicable Mathematics*. MacMillan, London (1973).

SUR UN MODELE DE LA PERIODE DE FROTTEMENT DANS LE SOUDAGE DE TUBES FINS PAR FRICTION

Résumé—Le matériau amolli pendant la phase de frottement dans le processus de soudage par friction est modélisé par un fluide newtonien à viscosité grande (mais constante). Le raccourcissement axial est inclus et des solutions approchées, acceptables pour des tubes minces d'acier doux, sont obtenues à partir de la méthode du bilan thermique intégral.

EIN MODELL FÜR DIE REIBUNGSPHASE BEIM REIBUNGSSCHWEISSEN VON DÜNNEN ROHREN

Zusammenfassung—Das erweichte Material, das während der Reibungsphase beim kontinuierlich fortgeführten Reibungsschweißprozeß vorhanden ist, wird im Modell als Newtonsche Flüssigkeit mit großer (aber konstanter) Viskosität behandelt. Die axiale Verkürzung ist mit einbezogen, und Näherungslösungen für dünne Rohre aus nieder legiertem Stahl wurden durch Anwendung der Wärmebilanz-Integral-Methode ermittelt.

О МОДЕЛИ СВАРКИ ТРЕНИМ ТОНКИХ ТРУБ

Аннотация—Размягченный материал, возникающий обычно в процессе сварки трением, представляется моделью ньютоновской жидкости с большой (но постоянной) вязкостью. При помощи интегрального метода теплового баланса найдены приближенные решения, пригодные для тонких труб из мягких сталей, учтено аксиальное укорочение.